A Relationship Between the Glass Transition Temperature (T_g) and Fractional Conversion for Thermosetting Systems

R. A. VENDITTI,[1] J. K. GILLHAM[2]

[1]Department of Wood and Paper Science, North Carolina State University, Box 8005, Raleigh, North Carolina 27695-8005

[2]Polymer Materials Program, Department of Chemical Engineering, Princeton University, Princeton, New Jersey 08544

Received 6 March 1996; accepted 7 May 1996

ABSTRACT: An equation, based on thermodynamic considerations to relate the glass transition temperature, T_g, to compositional variation of a polymer system, is adapted in this article for modeling the T_g vs. fractional conversion (x) relationship of reactive thermosetting systems. Agreement between the adapted equation and experimental T_g vs. x data is found for several thermosetting crosslinking systems (i.e., epoxies and cyanate ester/polycyanurate) as well as for reactive thermosetting linear polymer systems (i.e., polyamic acid and esters to polyimides). The equation models the experimentally obtained T_g vs. x behavior of thermosetting systems which include competing reactions. Agreement for widely varying molecular structures demonstrates the generality of the equation. The entire T_g vs. x relationship can be predicted for a thermosetting material by using the T_g vs. x equation and the values of the initial glass transition temperature, T_{g0}, the fully reacted system glass transition temperature, $T_{g\infty}$, and the ratio of the change in specific heat from the liquid or rubbery state to the glassy state (Δc_p) at T_{g0} and $T_{g\infty}$, $\Delta c_{p\infty}/\Delta c_{p0}$. The values of T_{g0}, $T_{g\infty}$, and $\Delta c_{p\infty}/\Delta c_{p0}$ can be measured generally from two differential scanning calorimetric experiments. © 1997 John Wiley & Sons, Inc. J Appl Polym Sci **64:** 3–14, 1997

INTRODUCTION

The glass transition temperature, T_g, is the most important material parameter of a glass. The glass transition temperature marks the temperature boundary of significant changes in the viscoelastic, dilatometric, enthalpic, etc., properties of all glass-forming materials. The relationship between T_g and fractional chemical conversion, x, for thermosetting materials, is a central concept in analyzing cure phenomena. As examples of the relevance of T_g to processing and properties, (1) the processing of a reactive material must be performed at temperatures above the value of T_g of the uncured material, T_{g0}, so that the material can be conveniently applied in a state of low viscosity and (2) the value of T_g at full conversion of a thermoset, $T_{g\infty}$, is related to the upper temperature limit of the material as a glass.

The relationship between T_g and fractional conversion determines when solidification (vitrification) occurs during cure, for which T_g equals the cure temperature (T_{cure}). At a given T_{cure}, the reaction of a thermosetting material proceeds generally at a rate dictated by chemical kinetics if T_g is less than T_{cure}; however, if T_g is greater than T_{cure}, the reaction rate may decrease by orders of magnitude due to a relative lack of mobility of the reactive groups.[1] The cure process is conveniently presented in an isothermal time–temperature–

Correspondence to: R. A. Venditti.

 CCC 0021-8995/97/010003-12

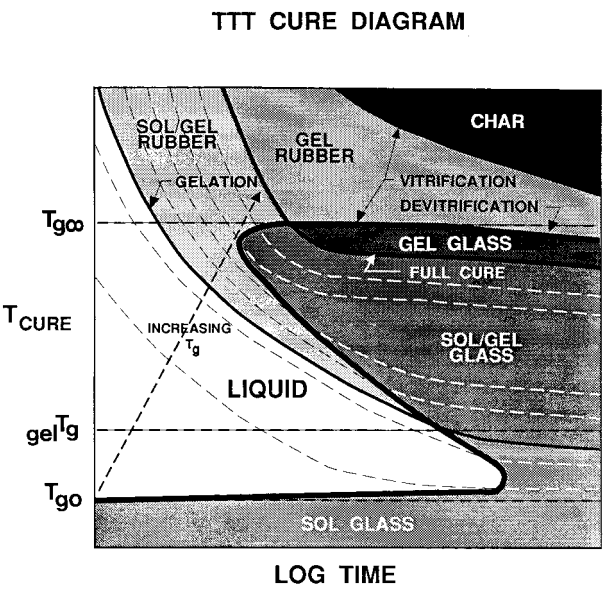

Figure 1 Generalized TTT isothermal cure diagram. Gelation, vitrification, and isoconversion (equivalently, iso-T_g) contours are shown. Reproduced with permission from the *J. Appl. Polym. Sci.,* **41,** 2885–2929 (1990).

transformation (TTT) cure diagram,[1–6] which displays gelation and vitrification contours vs. time (Fig. 1). An S-shaped vitrification contour and the gelation contour dominate the isothermal curing behavior of the thermoset. (In a simple system, gelation occurs at a particular conversion and, thus, at a particular T_g, designated gel T_g.) Hence, it is imperative to know the T_g vs. conversion relationship when modeling the cure of a thermoset or designing an optimum cure schedule.

Theoretical approaches for modeling the T_g vs. conversion relationship have been presented for thermosetting materials.[1,5–11] Complications in the use of some of the resulting equations include mathematical complexity and/or multiple fitting parameters that must be determined from rigorous experiments or from actually fitting the T_g vs. conversion data.

It is proposed to adapt an equation as derived by Couchman to predict the T_g vs. compositional variation of a polymer system[12,13] to model the T_g vs. conversion relationship for thermosetting systems. The T_g vs. conversion behavior for a thermosetting system can be predicted by using the adapted equation and differential scanning calorimetric (DSC) measurements on the uncured and on the fully cured material. The equation is tested by measurements of T_g vs. conversion for several thermosetting systems. The equation has parameters which are easily measurable for many materials and which have clear meanings, has application to a wide variety of polymer systems, and has a relatively simple mathematical form. A preliminary report has been published.[14] A fuller account appears in Ref. 15.

T_g vs. Conversion Relationship

The following derivation was presented by Couchman to predict the T_g vs. compositional variation of a polymer system[12,13]; the same procedure will be applied in this section to the T_g vs. fractional conversion of thermosetting systems.

Consider a thermosetting material that has some arbitrary fractional conversion, x, of the limiting reactant. The symbols 0 and ∞ are used to denote the uncured material and fully cured material, respectively. The system at conversion, x, is assumed to be a random mixture of unreacted end segments with concentration $1 - x$ and associated $T_g = T_{g0}$ and reacted end segments with concentration x and associated $T_g = T_{g\infty}$. The pure component entropies of the unreacted end segments and reacted end segments are denoted as S_0 and S_∞. The mixed system molar entropy, S, can thus be written as

$$S = (1 - x)S_0 + xS_\infty + \Delta S_m \qquad (1)$$

where ΔS_m is the excess entropy of mixing. The entropies of the unreacted and reacted end segments (S_0 and S_∞) at a given temperature, T, are related to their entropies at their respective values of T_g, i.e., S_0^0 at T_{g0} and S_∞^0 at $T_{g\infty}$. The following equation may be constructed from basic thermodynamic definitions:

$$S = (1 - x)\left(S_0^0 + \int_{T_{g0}}^{T} c_{p0}\, d \ln T\right) + x\left(S_\infty^0 + \int_{T_{g\infty}}^{T} c_{p\infty}\, d \ln T\right) + \Delta S_m \qquad (2)$$

where c_{p0} and $c_{p\infty}$ are the specific heat capacities at constant pressure at $x = 0$ and $x = 1$, respectively. The mixed system T_g is defined by the requirement that S in the glassy state is equal to S in the liquid/rubbery state:

$$(1-x)\left(S_0^{0,g}+\int_{T_{g0}}^{T_g} c_{p0}^{g} d\ln T\right) + x\left(S_\infty^{0,g}+\int_{T_{g\infty}}^{T_g} c_{p\infty}^{g} d\ln T\right) + \Delta S_m^{g} = (1-x)\left(S_0^{0,l}+\int_{T_{g0}}^{T_g} c_{p0}^{l} d\ln T\right) + x\left(S_\infty^{0,l}+\int_{T_{g\infty}}^{T_g} c_{p\infty}^{l} d\ln T\right) + \Delta S_m^{l} \quad (3)$$

where the superscripts l and g denote the liquid/rubbery state and glassy state, respectively. The choice of pure component reference states at T_{g0} and $T_{g\infty}$ provides the identities that $S_0^{0,g} = S_0^{0,l}$ and $S_\infty^{0,g} = S_\infty^{0,l}$. Further, the excess mixing entropy is continuous with respect to temperature at T_g.[12] Simplifying and regrouping,

$$(1-x)\left(\int_{T_{g0}}^{T_g} (\Delta c_{p0}) d\ln T\right) + x\left(\int_{T_{g\infty}}^{T_g} (\Delta c_{p\infty}) d\ln T\right) = 0 \quad (4)$$

where $\Delta c_{p0} = c_{p0}^{l} - c_{p0}^{g}$ and $\Delta c_{p\infty} = c_{p\infty}^{l} - c_{p\infty}^{g}$ for $x = 0$ and $x = 1$, respectively. In some cases, it may be approximated[12] that Δc_p is a constant with respect to temperature for a fixed conversion (i.e., $x = 0$ and $x = 1$); this approximation will be discussed in the Results and Discussion section. Finally, by integrating eq. (4) and solving for the natural logarithm of T_g,

$$\ln(T_g) = \frac{(1-x)\ln(T_{g0}) + \dfrac{\Delta c_{p\infty}}{\Delta c_{p0}} x \ln(T_{g\infty})}{(1-x) + \dfrac{\Delta c_{p\infty}}{\Delta c_{p0}} x} \quad (5)$$

where temperatures are in Kelvin. The above equation will be tested for thermosetting crosslinking systems (e.g., aromatic epoxy/aromatic amine,[1,5] aromatic epoxy/novolac,[8] and cyanate ester/polycyanurate[6]) by determining if eq. (5) fits experimental T_g vs. x data. It will also be determined if the best-fit parameter of $\Delta c_{p\infty}/\Delta c_{p0}$ from eq. (5) agrees with independently measured DSC values.

The equation will also be used to fit T_g vs. x data for thermosetting linear poly(amic acid) (and ester)/polyimide-type systems[16,17] that do not crosslink, but whose T_g rises largely from the formation of molecularly stiff semiladder-type polymer segments from linear polymer.[16–22] For these systems, the subscripts in eq. (5), 0 and ∞, denote the uncured and fully cured linear polymer properties, respectively. For the partially cured materials, the systems may be modeled as copolymers of unreacted segments [poly(amic acid) or ester with mol fraction = $1 - x$] and reacted segments (polyimide with mol fraction = x). For these systems, eq. (5) is the same as the original equation Couchman derived to relate T_g to compositional variations in linear copolymers where x and $(1 - x)$ are the mol fractions of the two comonomers.[12,13]

Pascault and Williams[7] used eq. (4) above and assumed that $\Delta c_{p0}(T) = \Delta c_{p0}|_{T=T_{g0}} \cdot \dfrac{T_{g0}}{T}$ and $\Delta c_{p\infty}(T) = \Delta c_{p\infty}|_{T=T_{g\infty}} \cdot \dfrac{T_{g\infty}}{T}$ for a fixed conversion and arrived at eq. (6):

$$T_g = \frac{(1-x)T_{g0} + \lambda x T_{g\infty}}{(1-x) + \lambda x} \quad (6)$$

or, equivalently,

$$\frac{T_g - T_{g0}}{T_{g\infty} - T_{g0}} = \frac{\lambda x}{1 - (1-\lambda)x} \quad (6)$$

where $\lambda = \Delta c_{p\infty}/\Delta c_{p0}$. Values of λ, from the best fit of eq. (6) to T_g vs. x data, will also be compared in this report to values of $\Delta c_{p\infty}/\Delta c_{p0}$ determined by DSC. Equation (6) is the same as the DiBenedetto equation.[7,10]

Note that the derivations of eq. (5) and eq. (6) are different only after eq. (4). For the derivation of eq. (5), Δc_{pi} ($i = \infty$ or 0) is estimated to be a constant with respect to temperature, $\Delta c_{pi}(T) = \Delta c_{pi}(T_g)$, and is substituted into eq. (4). For the derivation of eq. (6), Δc_{pi} is substituted into eq. (4) with the form $\Delta c_{pi}(T) = \Delta c_{pi}|_{T=T_{gi}} \cdot \dfrac{T_{gi}}{T}$. To determine the appropriateness of each derivation, the above two assumptions pertaining to Δc_{pi} must be further explored. This can be done experimentally by determining the dependence of Δc_{pi} on temperature or by locating data in the literature. This work is ongoing. (More is said pertaining to this matter in the Results and Discussion section of this article.)

Equation (6) has the identical mathematical

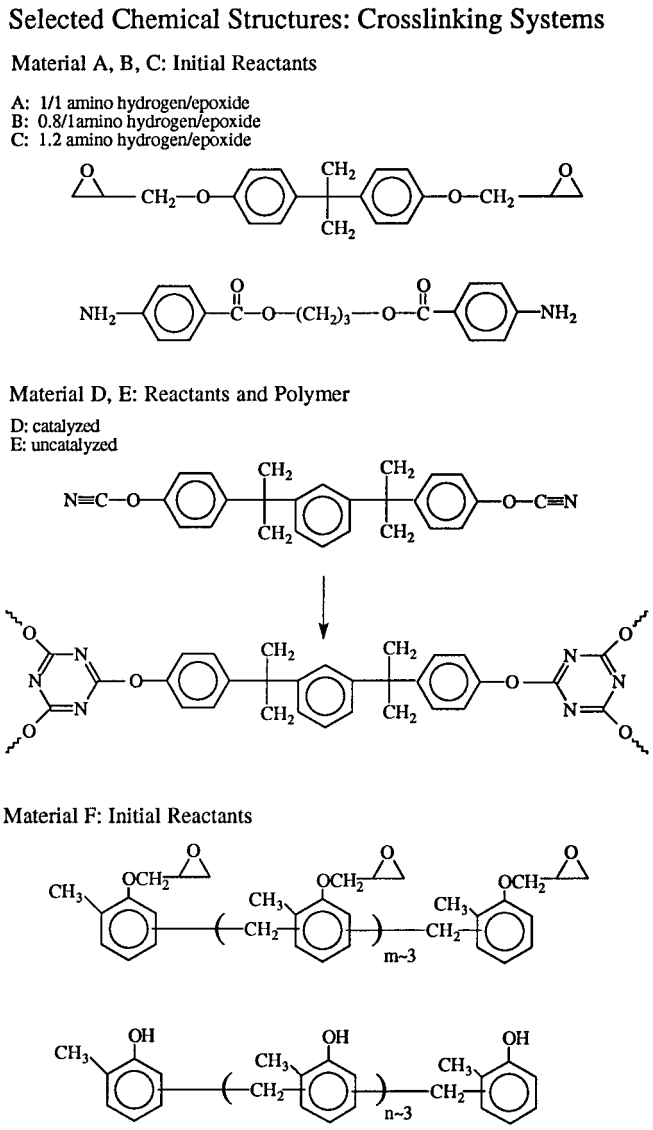

Figure 2 (A) Selected chemical structures: crosslinking systems. (B) Selected chemical structures: polyimide systems.

form as an equation derived by Gordon and Taylor using volumetric arguments to predict the value of T_g of a linear random copolymer with repeat units A and B vs. mol fraction of A and B,[23] where T_{g0} and $T_{g\infty}$ correspond to T_{gA} and T_{gB}, respectively. Comparison of eq. (6) with the Gordon–Taylor equation reveals that the parameter λ in eq. (6) is equal to the quantity $\Delta\alpha_A/\Delta\alpha_B$ in the Gordon–Taylor equation, where $\Delta\alpha$ is the difference in the thermal expansion coefficient between the liquid/rubbery state and the glassy state for a homopolymer consisting of A or B. If it is assumed that the Gordon–Taylor equation is applicable to the T_g vs. x data of a thermosetting material, then λ is taken to equal $\Delta\alpha_\infty/\Delta\alpha_0$, where ∞ and 0 denote the fully cured material and uncured material, respectively.

It is of interest to note that the relationship between T_g and conversion in eqs. (5) and (6) was derived by using general thermodynamic arguments, e.g., by equating the entropy of the liquid with the entropy of the glass at the glass transition. Information on structural features of the molecular architecture vs. conversion are not necessary to utilize eqs. (5) and (6). For example, the crosslink density, molecular weight, and the conversion at gelation are not used in the equation. Accordingly, it is expected that this equation is

Material G: Uncured and Fully-cured Polymer

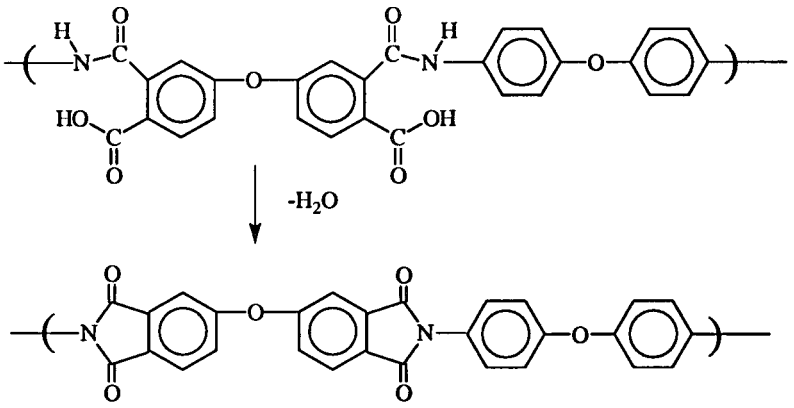

Material H: Fully-cured Polymer From Polyamic Acid

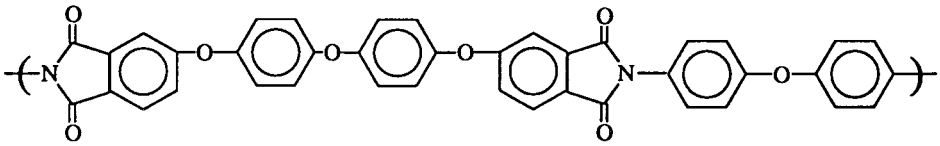

Material I: Uncured and Fully-cured Polymer

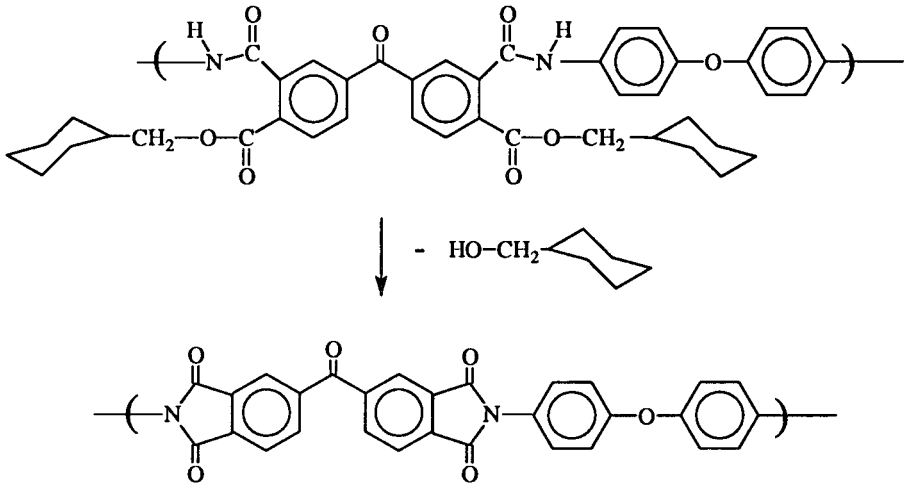

Figure 2 (*Continued from the previous page*)

general in its scope, capable of fitting T_g vs. conversion for a wide variety of thermosetting structures.

The generality of eqs. (5) and (6) may be contrasted to other T_g vs. conversion relationships for thermosetting systems which are derived by explicitly accounting for the effects of changes in molecular architecture on the value of T_g.[1,5,6,8,9,11] For example, Aronhime and Gillham[11] calculated a T_g vs. conversion relationship by separating the contributions of the sol and gel fractions to the overall T_g of a thermosetting system:

$$T_g = w_s T_{gs} + w_g T_{gg} \tag{7}$$

where w_s and w_g are the sol and gel weight fractions, respectively, and T_{gs} and T_{gg} are the values of T_g of the sol and gel fractions, respectively. The value of T_{gs} was related to the number-average molecular weight of the sol and the value of T_{gg}

was related to the crosslink density of the gel; thus, features of the molecular architecture must be known to utilize this equation. Equation (7) is also the basis for the equations used in Refs. 1, 5, 6, 8, and 9.

The advantage of using an equation based on structural features is that an understanding of the effect of structural features on T_g may be acquired. However, the mathematical complexity, the multiple structural parameters, the uncertainties of the actual evolving chemical structure vs. T_g in the thermosetting material under investigation, and the fitted or estimated parameters of such equations can prohibit the clear determination of structure vs. T_g relationships for all but the simplest systems.

EXPERIMENTAL

The T_g vs. x experimental data were obtained in this laboratory[1,5,6,15,16,24] or retrieved from the literature.[8,17] Selected chemical structures of the thermosetting materials are shown in Figure 2(A) and (B); the materials are labeled for convenience with the letters A–I. Various techniques for determining the values of T_g and conversion were utilized by the different authors. Measurements of conversion were performed by infrared spectroscopy, differential scanning calorimetry (DSC), and dynamic mechanical analysis as described in the references. T_g values were determined by differential scanning calorimetry, thermomechanical, or dynamic mechanical analysis as described in the references.

When measuring the fractional conversion from the residual heat in a DSC scan, $c_p(T)$ is almost always assumed to be constant with respect to x (e.g., as in Ref. 1). However, this assumption is not necessary in using the relatively new modulated DSC (MDSC) technique; changes in $c_p(T)$ with x can be quantitatively determined, even during periods where reaction occurs. Future work will include ascertaining if MDSC data produce T_g vs. x relationships different from those obtained from conventional DSC data. MDSC scans should provide better data than can conventional DSC to determine Δc_{p0} and $\Delta c_{p\infty}$ vs. temperature.

The experimental procedure for the determination of the T_g vs. conversion data for the poly(amic acid)ester/polyimide system which has methylcyclohexyl alcohol as the leaving group has been described by the authors of this report.[16] Details of the poly(amic acid)ester synthesis are available.[19,20]

RESULTS AND DISCUSSION

Dependence of Δc_p on Temperature

In the derivation of eq. (5), it was assumed/approximated that Δc_{p0} and $\Delta c_{p\infty}$ are constant (but different) with respect to temperature. The following discusses certain aspects of this assumption:

DSC scans of material A, which contains the stoichiometric ratio of amino hydrogens to epoxide groups, for different conversion values of x from 0 to 1 are shown in Figure 3.[1] It can be observed that, in the absence of a transition or reaction, c_p (which equals a constant times mcal/s in Fig. 3) varies approximately linearly with temperature in the glassy state and in the liquid/rubbery state at a given conversion for all conversions.

Using this observation, c_p for the liquid/rubbery state and for the glassy state, for a given value of conversion (i.e., T_g), can be written as follows:

$$c_p^l(T_g, T) \cong c_p^l(T_g) + m_p^l(T - T_g) \qquad (8)$$

$$c_p^g(T_g, T) \cong c_p^g(T_g) + m_p^g(T - T_g) \qquad (9)$$

where $c_p(T_g, T)$ depends on both the conversion of the material, as reflected by its T_g, and the measurement temperature. The parameter m_p is simply the slope of c_p vs. temperature for the glassy state or liquid/rubbery state in a temperature range which is unaffected by transitions or reactions:

$$m_p^i = \frac{dc_p^i}{dT} \cong \text{constant} \qquad (10)$$

where i may be either l or g. Subtracting eq. (9) from eq. (8) results in the Δc_p as a function of conversion (i.e., T_g) and measurement temperature:

$$\Delta c_p(T_g, T) \cong [c_p^l(T_g) - c_p^g(T_g)] + (m_p^l - m_p^g)(T - T_g) \qquad (11)$$

Note that eq. (11) shows Δc_p to be an approximately linear function of temperature at a given value of conversion (i.e., T_g). The value of m_p^g is generally greater than m_p^l. Therefore, Δc_p is ex-

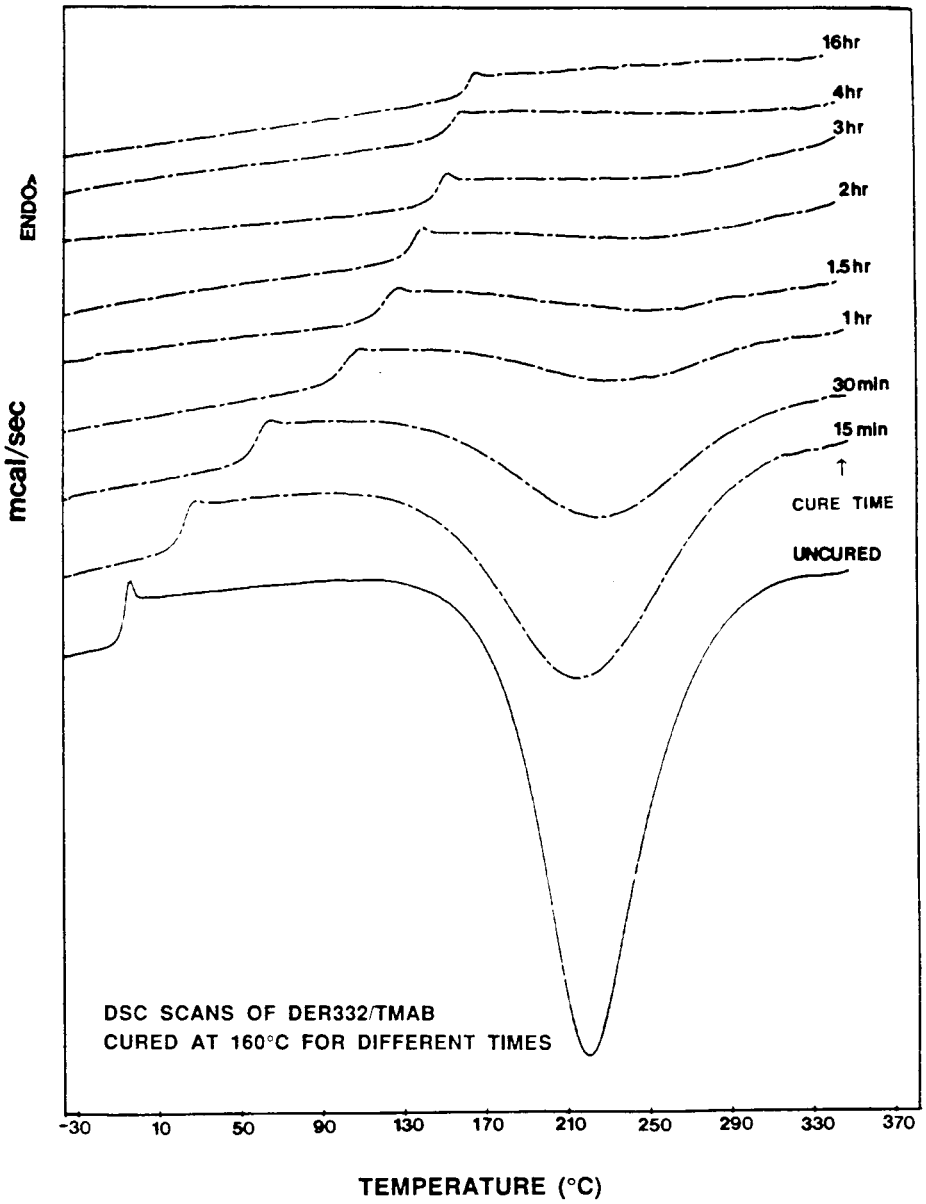

Figure 3 DSC scans for material A (diepoxy-tetrafunctional diamine) at different conversions.[1] Data were shifted vertically for purposes of clarity. Reproduced with permission from the *J. Appl. Polym. Sci.,* **41,** 2885–2929 (1990).

pected to decrease linearly with increasing temperature at a fixed conversion. This is in contrast to the inverse relationship between Δc_p and T used to obtain eq. (6).

The form of $\Delta c_p(T_g, T)$ as written in eq. (11) for materials with conversions of $x = 0$ and $x = 1$ may be substituted into eq. (4). However, the results of this article (see later) show good agreement between the simplified eq. (5), using $\Delta c_p(T_g, T)$ equal to a constant for conversions $x = 0$ and $x = 1$ and observed T_g vs. x data. Further, the value of $m_p^l - m_p^g$ is experimentally more difficult to quantify to the same accuracy as Δc_p using DSC. Including an inaccurate measurement of $m_p^l - m_p^g$ may then detract from the comparison between eq. (4) and experimental results.

Use of the MDSC technique should permit the quantitative determination of values of m and, more broadly, provide the functional relationship between Δc_p and T and x. Future work using the MDSC technique will be performed on this issue.

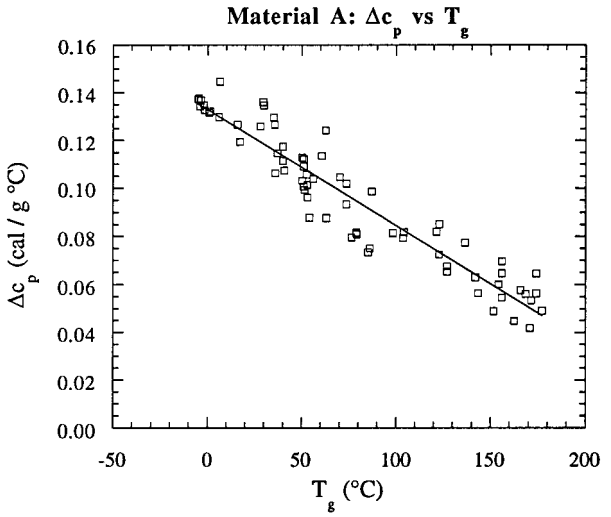

Figure 4 Δc_p vs. T_g for material A (diepoxy-tetrafunctional diamine). Data from Ref. 15.

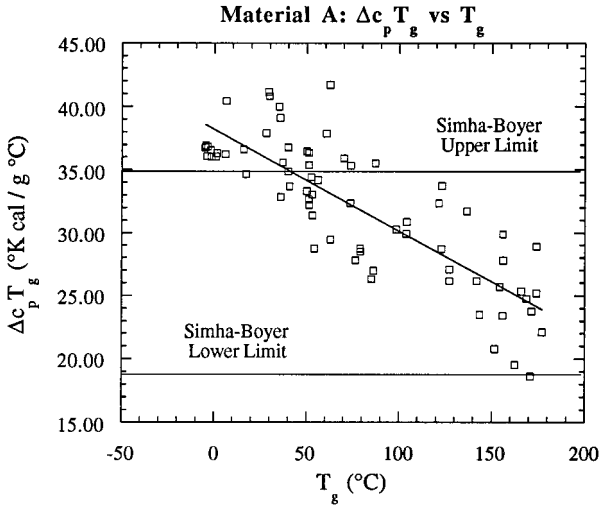

Figure 5 $\Delta c_p T_g$ vs. T_g for material A (diepoxy-tetrafunctional diamine). Simha–Boyer limits are also drawn. Data from Ref. 15.

Dependence of Δc_p at T_g on Conversion

Simha and Boyer[25] postulated the following approximate generalization:

$$\Delta c_p(T_g, T = T_g)T_g = b$$

or

$$\Delta c_p(T_g, T = T_g) = \frac{b}{T_g} \qquad (12)$$

where Δc_p is measured at a temperature equal to T_g and b is a constant for all amorphous materials. Equation (12) is an approximation. For example, Figures 4 and 5 (Ref. 15) display Δc_p vs. T_g and $\Delta c_p T_g$ vs. T_g for material A, respectively. Δc_p decreases with increasing T_g or, equivalently, conversion (Fig. 4). The values of $\Delta c_p T_g$ lie within the upper and lower Simha–Boyer limits for b at conversions greater than $T_g \approx 100$°C (Fig. 5); however, the values of $\Delta c_p T_g$ show a significant decreasing trend in Figure 5.

Note that eqs. (12) describe the dependence of Δc_p measured at the temperature T_g on the conversion, T_g; eqs. (12) do not predict the dependence of Δc_p on temperature at a fixed conversion, i.e., fixed T_g. The functionality of Δc_p on temperature at a fixed T_g is required for substitution of Δc_p in eq. (4). Thus, it is not appropriate to invoke the Simha–Boyer rule, i.e., eq. (12), for substitution of Δc_p in eq. (4).

Comparison of Fitted and Experimental Values of $\Delta c_{p\infty}/\Delta c_{p0}$

Figures 6–11 display some of the experimentally obtained sets of T_g vs. x data. For each set, the data were fitted using the least-squares method to eq. (5) and to eq. (6) to yield the parameters T_{g0}, $T_{g\infty}$, and $\Delta c_{p\infty}/\Delta c_{p0}$. The fit of the data to eq. (5) is shown for several polymer systems in Figures 6–11 [the fit of the data to eq. (6) is not shown]. The best-fit values of $\Delta c_{p\infty}/\Delta c_{p0}$ using eqs. (5) and (6) are reported in Table I for the crosslinking thermosetting materials and in Table II for the linear polyimide-type thermosetting materials. Table I also includes independently measured values of $\Delta c_{p\infty}/\Delta c_{p0}$ from DSC analysis. The correlation coefficient, R, which was calculated using the Kaleidagraph graphing software program for the Macintosh computer, for each fit is also shown in Tables I and II.

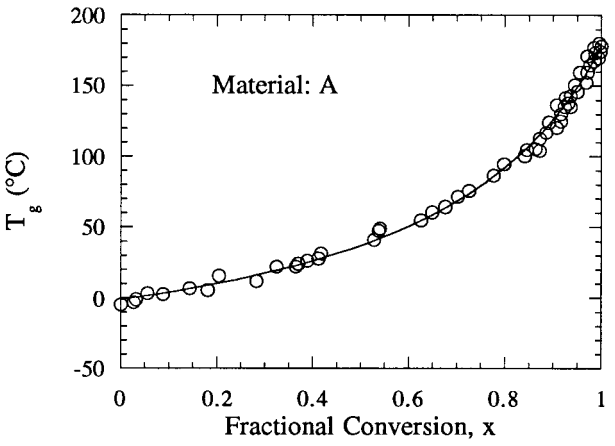

Figure 6 T_g vs. x for material A (diepoxy-tetrafunctional diamine, stoichiometric ratio). Data from Ref. 1.

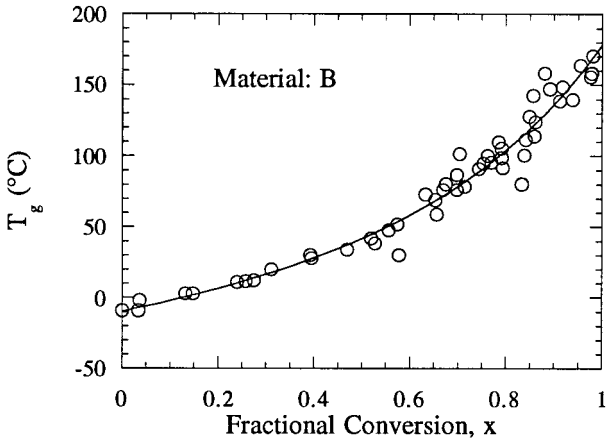

Figure 7 T_g vs. x for material B (diepoxy-tetrafunctional diamine, excess of epoxy). Data from Ref. 5.

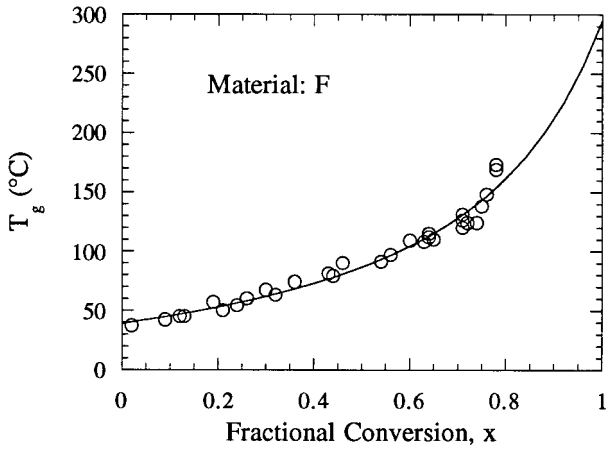

Figure 9 T_g vs. x for material F (epoxy cresol novolac–cresol novolac hardener). Data from Ref. 8.

Figures 6–11 show that eq. (5) fits all the sets of data well, as reflected in the values of the correlation coefficient. The results in Table I show quantitative agreement between the best-fit value of $\Delta c_{p\infty}/\Delta c_{p0}$ using eq. (5) and the independently DSC measured value for a variety of different systems (data collected by various researchers). The agreement demonstrates the generality of eq. (5). Its utility in characterizing the T_g vs. x behavior of new materials is that by performing only two straightforward DSC experiments, one on the uncured and one on the fully cured material, the entire T_g vs. conversion relationship may be predicted. The resulting eq. (5) is also in a mathematical form that is simple and convenient to incorporate into a more complex model, e.g., in one used to calculate the vitrification contour in the time–temperature–transformation isothermal cure diagram.[1,2,11]

Equation (6) also fits the T_g vs. x data well (plots not shown; see the values of the correlation coefficient in Tables I and II). The values of $\lambda = \Delta c_{p\infty}/\Delta c_{p0}$ determined by fitting the data to eq. (6) follow the same trend as do the measured DSC values of $\Delta c_{p\infty}/\Delta c_{p0}$ but are significantly lower than the measured DSC values. On this basis, eq. (5) appears to be a better predictive tool than eq. (6).

Diepoxy/tetrafunctional Diamine (Materials A, B, and C)

For the stoichiometric (i.e., amino hydrogen/epoxide group = r = 1.0) system (material A, Fig. 6) and the amine-rich system (material C: r = 1.2, data[5] not shown here), there are reactions between primary and secondary amino hydrogens

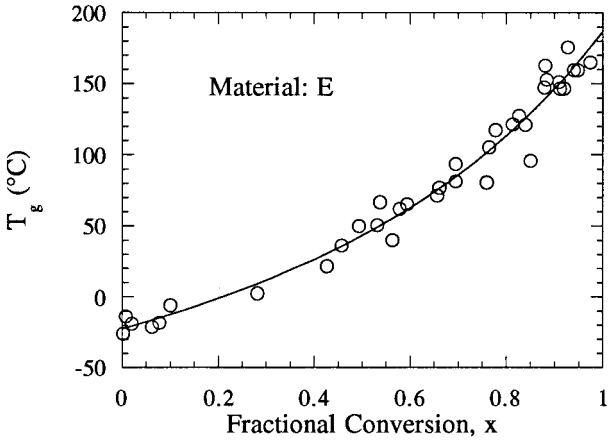

Figure 8 T_g vs. x for material E (dicyanate ester to polycyanurate, uncatalyzed system). Data from Ref. 6.

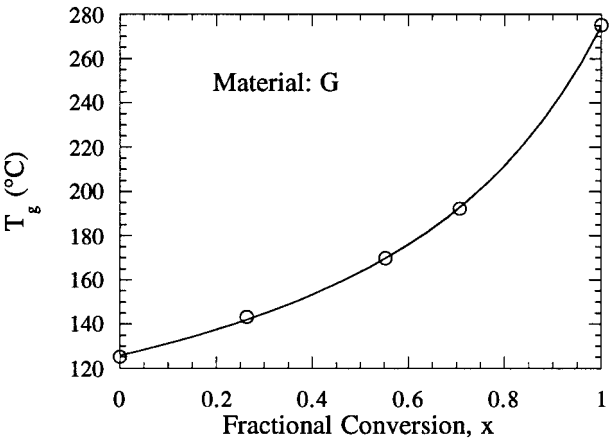

Figure 10 T_g vs. x for material G [poly(amic acid) to polyimide]. Data from Ref. 17.

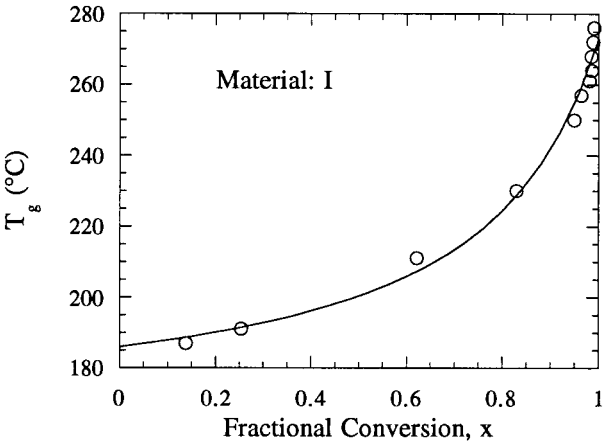

Figure 11 T_g vs. x for material I [poly(amic acid)ester to polyimide]. Data from Ref. 16.

and epoxide[1]; for the epoxy-rich system (material B: $r = 0.8$, Fig. 7), an additional reaction occurs between the excess epoxy and hydroxyl groups generated by epoxy/amine reactions.[5] Equation (5) adequately fits the data without regard to the relative rates of the different types of reactions (which have different reaction rate constants[26]).

It has been shown that the T_g vs. x relationship, despite competing reactions, is unique, independent of cure path (time–temperature history) for the three stoichiometric ratios studied for this system.[1,5,26,27] This is also true for all of the crosslinked systems investigated in this report. This suggests that the T_g is not sensitive to the chemical identity of a crosslink other than the way that a crosslink affects the entropy of the system, as described in eq. (5). The insensitivity of the T_g vs. x relationship has been discussed.[9]

Dicyanate Ester/Polycyanurate (Materials D and E)

Both the catalyzed system (material D: 1.96 wt % copper naphthenate and nonylphenol, data[6] not shown here) and uncatalyzed system (material E, Fig. 8) show the same T_g vs. x behavior when normalized for the differences in T_{g0} and $T_{g\infty}$.[6] (The differences in T_{g0} and $T_{g\infty}$ for the catalyzed and uncatalyzed systems are the consequence of plasticization by the catalyst.) Further, the T_g vs. conversion data for each system overlap for samples cured at different T_{cure}. Thus, T_g may be assumed to be independent of the reaction pathway in which the material arrived at its conversion.

Epoxy/Novolac (Material F)

The epoxy cresol novolac and cresol novolac hardener system included a 0.74 wt % imidazole accelerator (material F, Fig. 9). The T_g vs. conversion data for this system are not available for $x > 0.80$. It is possible to induce higher conversions in this system by using longer cure times and higher cure temperatures than those used in the reported study,[8] although competition between cure and thermal degradation will probably complicate the results for reactions above 200°C. The value of $\Delta c_{p\infty}$ is approximated as the measured value at $x = 0.78$ (rather than at $x = 1$). This approximation was based on an extrapolation of the reported Δc_p vs. conversion data for this system, in spite of the large scatter of the data at high conversion.[8] It is also of interest to note that no effect on the T_g vs. x relationship of this material was observed for different cure paths (time–temperature sequence).[8]

Table I Thermosetting (Crosslinked) Systems: Predicted and Measured $\Delta c_{p\infty}/\Delta c_{po}$ Values

Material	$\Delta c_{p\infty}/\Delta c_{po}$ DSC[a]	$\Delta c_{p\infty}/\Delta c_{po}$ Eq. (5)[b]	R[c] Eq. (5)	$\Delta c_{p\infty}/\Delta c_{po}$ Eq. (6)[d]	R[e] Eq. (6)	Ref.
A	0.35	0.35	1.00	0.26	1.00	1
B	0.5 ± 0.1	0.50	0.99	0.39	0.99	5, 24
C	0.5 ± 0.1	0.50	0.98	0.39	0.98	5, 24
D	0.6 ± 0.1	0.58	0.99	0.44	0.99	6
E	0.6 ± 0.1	0.62	0.99	0.46	0.99	6
F	0.3	0.31	0.99	0.16	0.98	8

[a] Measured value of $\Delta c_{p\infty}/\Delta c_{po}$ from DSC scans at $x = 0$ and $x = 1$.
[b] $\Delta c_{p\infty}/\Delta c_{po}$ from best fit of T_g vs. x data to eq. (5).
[c] Correlation coefficient (R) of least-squares fit of data to eq. (5).
[d] $\Delta c_{p\infty}/\Delta c_{po}$ from best fit of T_g vs. x data to eq. (6).
[e] Correlation coefficient (R) of least-squares fit of data to eq. (6).

Table II Poly(amic acid) (or Ester)/Polyimide Systems: Predicted $\Delta c_{p\infty}/\Delta c_{po}$ Values

Material	$\Delta c_{p\infty}/\Delta c_{po}$ Eq. (5)[a]	R[b] Eq. (5)	$\Delta c_{p\infty}/\Delta c_{po}$ Eq. (6)[c]	R[4] Eq. (6)	Ref.
G	0.40	1.00	0.34	1.00	17
H	0.65	1.00	0.56	1.00	17
I	0.22	0.99	0.19	0.99	16

[a] $\Delta c_{p\infty}/\Delta c_{po}$ from best fit of T_g vs. x data to eq. (5).
[b] Correlation coefficient of least-squares fit of data to eq. (5).
[c] $\Delta c_{p\infty}/\Delta c_{po}$ from best fit of T_g vs. x data to eq. (6).
[d] Correlation coefficient (R) of least-squares fit of data to eq. (6).

Linear Poly(amic acid) (or Ester)/Polyimide (Materials G, H, and I)

For the linear poly(amic acid) (or ester)/polyimide systems values of $\Delta c_{p\infty}/\Delta c_{p0}$ are not available from DSC measurements at $x = 0$ and $x = 1$. At low conversions, the value of Δc_{p0} is obscured during a DSC scan by the heat associated with the reaction; at high conversions, the value of $\Delta c_{p\infty}$ is so small that it is usually undetectable in a DSC scan. However, relative magnitudes of the expected values of $\Delta c_{p\infty}/\Delta c_{p0}$, estimated from the chemical structures of the fully cured materials and uncured materials, can be made and compared to the best-fit values of $\Delta c_{p\infty}/\Delta c_{p0}$ from the T_g vs. x data.

The magnitude of Δc_p reflects the difference in degrees of freedom (motion) between the liquid/rubbery state and the glassy state. In stiff molecular systems, the number of degrees of freedom in the liquid state is small, approaching the degrees of freedom in the glass; therefore, Δc_p is small. For nonstiff systems, the number of degrees of freedom is large in the liquid state relative to the glassy state; therefore, Δc_p is large.

The effect of molecular stiffness on Δc_p can be observed in Figure 4 for material A. At low values of T_g (or, equivalently, conversion), where the material has no crosslinks and low molecular weight (relatively nonstiff molecules), Δc_p is large. As T_g (or equivalently, x) increases, the stiffness of the molecular structure increases due to higher molecular weight and crosslinks. The value of Δc_p is observed to decrease with conversion (stiffness). Thus, the relative values of $\Delta c_{p\infty}/\Delta c_{p0}$ for two reactive systems can be estimated qualitatively by comparing the stiffness of the uncured and fully cured structures of the two systems.

Materials G (Fig. 10) and I (Fig. 11) have almost identical fully cured structures so their $\Delta c_{p\infty}$ values may be assumed to be equal. However, unreacted material I contains sequences of mobile nonpolar methylene groups which should increase the Δc_{p0} value relative to unreacted material G, which has acid groups that can participate in hydrogen bonding, effectively decreasing submolecular mobility. Thus, from the chemical structures alone, it is expected that $\Delta c_{p\infty}/\Delta c_{p0}$ will be larger for material G than for material I; this agrees with the relative values of $\Delta c_{p\infty}/\Delta c_{p0}$ obtained from the fits of the T_g vs. x data (Table II).

Also, it is expected that the value of $\Delta c_{p\infty}/\Delta c_{p0}$ should be smaller for material G than for material H because material G has a relatively larger change in overall submolecular stiffness from the uncured to fully cured state (i.e., more polyimide rings formed per repeat unit molecular weight) than has material H; this also is in agreement with the best-fit values of $\Delta c_{p\infty}/\Delta c_{p0}$ in Table II from eq. (5).

CONCLUSIONS

Equation (5) quantitatively models the T_g vs. x relationship for the thermosetting crosslinking systems and for the thermosetting linear polyimide-type systems studied. Agreement between the value of $\Delta c_{p\infty}/\Delta c_{p0}$ determined by fitting eq. (5) to experimental T_g vs. x data and the value obtained by independent DSC measurements demonstrate the utility of eq. (5). The findings of this article demonstrate that the T_g vs. x relationship is insensitive to the details of the changing chemical structure except for the way that the changing chemical structure alters the entropy of the system. The T_g vs. x relationship can be predicted for thermosetting materials by using eq. (5) and the values of T_{g0}, $T_{g\infty}$, and $\Delta c_{p\infty}/\Delta c_{p0}$, which can generally be measured from two DSC experiments. However, the advent of the modulated DSC tech-

nique should be applied to the problem of the T_g vs. conversion relationship so as to investigate the assumptions pertaining to the dependence of Δc_p on temperature invoked in the derivation of eq. (5).

REFERENCES

1. G. Wisanrakkit and J. K. Gillham, *J. Appl. Polym. Sci.,* **41,** 2885 (1990).
2. J. B. Enns and J. K. Gillham, *J. Appl. Polym. Sci.,* **28,** 2567 (1983).
3. S. L. Simon and J. K. Gillham, *J. Appl. Polym. Sci.,* **53,** 709 (1994).
4. S. Gan, J. K. Gillham, and R. B. Prime, *J. Appl. Polym. Sci.,* **37,** 803 (1989).
5. S. L. Simon and J. K. Gillham, *J. Appl. Polym. Sci.,* **46,** 1245 (1992).
6. S. L. Simon and J. K. Gillham, *J. Appl. Polym. Sci.,* **47,** 461 (1993).
7. J. P. Pascault and R. J. J. Williams, *J. Polym. Sci. Part B Polym. Phys.,* **28,** 85 (1990).
8. A. Hale, C. W. Macosko, and H. E. Bair, *Macromolecules,* **24,** 2610 (1991).
9. X. Wang and J. K. Gillham, *J. Appl. Polym. Sci.,* **45,** 2127 (1992).
10. A. T. DiBenedetto, *J. Polym. Sci. Part B Polym. Phys.,* **25,** 1949 (1987).
11. M. T. Aronhime and J. K. Gillham, *J. Coat. Technol.,* **56**(718), 35 (1984).
12. P. R. Couchman and F. E. Karasz, *Macromolecules,* **11,** 117 (1978).
13. P. R. Couchman, *Polym. Eng. Sci.,* **24**(2), 135 (1984).
14. R. A. Venditti and J. K. Gillham, in *Proceedings of the ACS: Polymer Materials: Science and Engineering Division,* Chicago, 1993, Vol. 69, pp. 434–435.
15. R. A. Venditti, PhD Thesis, Department of Chemical Engineering, Princeton University, 1994.
16. R. A. Venditti, J. K. Gillham, E. Chin, and F. M. Houlihan, *J. Appl. Polym. Sci.,* **53,** 455 (1994).
17. L. A. Laius, M. I. Bessonov, and F. S. Florinskii, *Vysok. Soyed,* **A13**(9), 2006 (1971).
18. R. A. Venditti, J. K. Gillham, E. Chin, and F. M. Houlihan, in *Advances in Polyimide Science and Technology,* C. Feger, Ed., Technomic, Lancaster, PA, 1993, pp. 336–350.
19. F. M. Houlihan, B. J. Bachman, C. W. Wilkins, Jr., and C. A. Pryde, *Macromolecules,* **22,** 4477 (1989).
20. E. Chin, F. M. Houlihan, R. A. Venditti, and J. K. Gillham, in *Advances in Polyimide Science and Technology,* C. Feger, Ed., Technomic, Lancaster, PA, 1993, pp. 201–212.
21. J. K. Gillham and H. C. Gillham, *Polym. Eng. Sci.,* **13**(6), 447 (1973).
22. M. I. Bessonov, M. M. Koton, V. V. Kudryavtsev, and L. A. Laius, *Polyimides: Thermally Stable Polymers,* Plenum, New York, 1987.
23. M. Gordon and J. S. Taylor, *J. Appl. Chem.,* **2,** 493 (1952).
24. S. Simon, private communication.
25. R. Simha and R. F. Boyer, *J. Chem. Phys.,* **37**(5), 1003 (1962).
26. X. Wang and J. K. Gillham, *J. Appl. Polym. Sci.,* **43,** 2267 (1991).
27. K. P. Pang and J. K. Gillham, *J. Appl. Polym. Sci.,* **37,** 1969 (1989).